Molecular Medicine

Bone-Targeting Endogenous Secretory Receptor for Advanced Glycation End Products Rescues Rheumatoid Arthritis

Tatsuo Takahashi,[1] Sayaka Katsuta,[1] Yusuke Tamura,[1] Nozomi Nagase,[1] Keita Suzuki,[1] Masaaki Nomura,[2] Shunji Tomatsu,[3,4] Ken-ichi Miyamoto,[5] and Shinjiro Kobayashi[1]

[1]Department of Clinical Pharmacy and [2]Educational Center of Clinical Pharmacy, Faculty of Pharmaceutical Sciences, Hokuriku University, Kanazawa, Japan; Departments of [3]Biomedical Research and [4]Pediatric Orthopedic Surgery, Nemours/Alfred I. duPont Hospital for Children, Wilmington, Delaware, United States of America; and [5]Department of Medicinal Informatics, Graduate School of Medical Sciences, Kanazawa University, Kanazawa, Japan

Rheumatoid arthritis (RA) is a chronic inflammatory synovitis that leads to the destruction of bone and cartilage. The receptor for advanced glycation end products (RAGE) is a multiligand membrane-bound receptor for high-mobility group box-1 (HMGB1) associated with development of RA by inducing production of proinflammatory cytokines such as tumor necrosis factor (TNF)-α, interleukin (IL)-1 and IL-6. We developed a bone-targeting therapeutic agent by tagging acidic oligopeptide to a nonmembrane-bound form of RAGE (endogenous secretory RAGE (esRAGE)) functioning as a decoy receptor. We assessed its tissue distribution and therapeutic effectiveness in a murine model of collagen-induced arthritis (CIA). Acidic oligopeptide–tagged esRAGE (D_6-esRAGE) was localized to mineralized region in bone, resulting in the prolonged retention of more than 1 wk. Weekly administration of D_6-esRAGE with a dose of 1 mg/kg to RA model mice significantly ameliorated inflammatory arthritis, synovial hyperplasia, cartilage destruction and bone destruction, while untagged esRAGE showed little effectiveness. Moreover, D_6-esRAGE reduced plasma levels of proinflammatory cytokines including TNF-α, IL-1 and IL-6, while esRAGE reduced the levels of IL-1 and IL-6 to a lesser extent, suggesting that production of IL-1 and IL-6 reduced along the blockade of HMGB1 receptor downstream signals by D_6-esRAGE could be attributed to remission of CIA. These findings indicate that D_6-esRAGE enhances drug delivery to bone, leading to rescue of clinical and pathological lesions in murine CIA.
Online address: http://www.molmed.org
doi: 10.2119/molmed.2012.00309

INTRODUCTION

Rheumatoid arthritis (RA) is a chronic inflammatory synovitis dominated by the presence of macrophages, lymphocytes and synovial fibroblasts, leading to the destruction of bone and cartilage (1). Uncontrolled active RA causes disability, decreases quality of life and increases morbidity. The introduction of novel biologics has revolutionized RA treatment.

Their success has underlined the key roles of proinflammatory cytokines in the pathogenesis of inflammatory arthritis, such as tumor necrosis factor (TNF)-α and interleukin (IL)-1 and IL-6 (2–4). Theoretically, this approach not only enhances the specificity in their effects but diminishes adverse events. Clinical studies on RA patients showed therapeutic efficacy by administering the agents

blocking TNF-α, IL-1 and IL-6, namely etanercept (5), anakinra (6) and tocilizumab (7), respectively. However, some patients did not respond to even such advanced biologic agents. Because the pathogenesis of RA is caused by multiple complex factors involving a wide range of molecules, the factors other than TNF-α, IL-1 and IL-6 also participate in the proinflammatory cytokine cascade.

Recent studies revealed that extracellular high-mobility group box 1 (HMGB1) levels in both serum and synovial fluid are significantly elevated in patients with RA (8,9). HMGB1 can bind to the cell surface receptors including toll-like receptor (TLR)-2, TLR-4 and the receptor for advanced glycation end products (RAGE) (10,11). HMGB1 interaction with these receptors transduces

intracellular signals and mediates the release of proinflammatory cytokines such as TNF-α in macrophages (9). Moreover, HMGB1 directly induces synovial cell proliferation and osteoclastogenesis, leading to the destruction of cartilage and bone (12–14). Thus, HMGB1 plays a critical role in the pathogenesis of RA and may become a putative target for successful RA treatment.

RAGE is composed of (a) an N-terminal extracellular domain with a ligand-engaging V-region–like domain essential for binding with HMGB1 and two C-region–like domains; (b) a single pass transmembrane domain; and (c) a C-terminal highly charged, short cytoplasmic domain essential for signal transduction (15–17). A soluble RAGE (sRAGE), a truncated form of the receptor, is composed of only the extracellular ligand-binding domain lacking the cytosolic and transmembrane domains. In humans, sRAGE is produced by alternative splicing of RAGE mRNA (18,19). Yonekura *et al.* (20) identified a naturally occurring sRAGE lacking transmembrane and intracellular domains in humans and named it endogenous secretory RAGE (esRAGE). This soluble form of the receptor is a C-terminally truncated type and has a V-domain essential for binding with the ligand such as HMGB1. Therefore, esRAGE has the same ligand binding specificity, competes with cell-bound RAGE for ligand binding and functions as a decoy abrogating cellular activation (20,21).

An innovative drug delivery system by using acidic oligopeptides to target bone was proposed and investigated experimentally and clinically (22–24). This unique approach is based on the physical properties of several noncollagenous bone proteins that have repetitive sequences of acidic amino acids (L-aspartic acid [L-Asp] or L-glutamine [L-Glu]) and bind to hydroxyapatite (HA) (25,26). It was indicated that the antibiotics fluoroquinolones, tagged with an acidic oligopeptide, were successfully targeted to bone and could be effective in treating osteomyelitis if the appropriate dose was given (24). We and

other groups have applied this bone-targeting system to large molecules, namely, enzymes (tissue-nonspecific alkaline phosphatase, β-glucuronidase and N-acetylgalactosamine-6-sulfate sulfatase), showing that the tagged enzymes were delivered more efficiently to bone and that the clinical and pathological improvement in bone was observed in murine models of hypophosphatasia, mucopolysaccharidosis VII and mucopolysaccharidosis IVA, respectively (27–30). The clinical trial for the patients with hypophosphatasia is now in progress with a favorable clinical consequence rescuing the devastating skeletal bone disease (31).

In this study, we applied and developed the bone-targeting drug delivery system for RA by tagging the acidic oligopeptide to esRAGE and evaluated the *in vivo* therapeutic effect of targeted esRAGE on the RA murine model.

MATERIALS AND METHODS

Mice and Reagents

Six-week-old male DBA/1J mice were purchased from Japan SLC (Hamamatsu, Japan). All mouse experiments were performed in accordance with the guidelines of the Committee on Animal Experiments at Hokuriku University.

Human lung total RNA was obtained from Clontech (Mountain View, CA, USA). Mammalian expression vector pcDNA3.1 (+), Lipofectamine 2000 and Alexa Fluor 488 Protein Labeling Kit were purchased from Invitrogen/Life Technologies (Carlsbad, CA, USA). Dulbecco's modified Eagle medium (DMEM) was from Nissui Pharmaceutical (Tokyo, Japan), and EX-CELL® 325 PF CHO Serum-Free Medium for CHO Cells (protein free) was obtained from SAFC Biosciences (Lenexa, KS, USA). G418, DEAE–Sepharose, Sephacryl S-300-HR and Nickel Affinity Gel were purchased from Sigma-Aldrich (St. Louis, MO, USA). Vivacell 70 and Vivaspin 15 centrifugal filter device were from Sartorius Stedim Biotech (Goettingen, Germany). Coomassie brilliant blue R-250, imidazole,

complete Freund adjuvant (CFA) and incomplete Freund adjuvant (IFA) were obtained from Wako (Osaka, Japan). Heparin Sepharose and ECL Plus kit were purchased from GE Healthcare (Chalfont St Giles, Buckinghamshire, UK). Detoxi-gel endotoxin removal gel was from Pierce (Rockford, IL, USA). Peptide N-glycosidase F (PNGase F) was obtained from New England Biolabs (Beverly, MA, USA). Primary anti-RAGE antibody was obtained from Santa Cruz Biotechnology (Santa Cruz, CA, USA), and secondary horseradish peroxidase–conjugated anti-rabbit IgG antibody was purchased from Cell Signaling (Beverly, MA, USA). HA beads were from Bio-Rad Laboratories (Richmond, CA, USA). Recombinant human HMGB1 was obtained from R&D Systems (Minneapolis, MN, USA), and His-tagged recombinant human HMGB1 was purchased from ATGen (Gyeonggi-do, Korea). Mouse monocyte/macrophage cell line RAW264.7 was from American Type Culture Collection (Manassas, VA, USA). Bovine collagen type II was obtained from Cosmo Bio (Tokyo, Japan). TNF-α enzyme-linked immunosorbent assay (ELISA) kit, IL-1 ELISA kit and IL-6 ELISA kit were purchased from R&D Systems.

Production of Untagged and Acidic Oligopeptide–Tagged Human Recombinant esRAGE (GenBank Accession No. AB061668)

To produce acidic oligopeptide–tagged esRAGE, a stretch of 6, 10 or 14 of L-Asp codons (6 L-Asp, 5′-GACGATGACG ACGATGAT-3′: 10 L-Asp, 5′-GACGA TGACGACGATGATGACGACGACGAC-3′: 14 L-Asp, 5′-GACGATGACGACGAT GATGACGACGACGACGATGATGATG AT-3′) was introduced additionally at the C-terminus after c.1041G of Met347 between the spacer (5′-ACCGGTGAAG CAGAGGCC-3′) and a termination codon. The esRAGE tagged with a stretch of 6, 10 and 14 of L-Asp were named D_6-esRAGE, D_{10}-esRAGE and D_{14}-esRAGE, respectively.

For preparation of the first-strand cDNA, reverse transcriptase reaction

was performed by using human lung total RNA. To amplify human esRAGE, D_6-esRAGE, D_{10}-esRAGE and D_{14}-esRAGE, polymerase chain reactions were carried out with the following primers: esRAGE forward 5'-ctcgagCCAGGACCCTGGAAGGAAGCAGGA-3' and reverse 5'-tctagaTTACATGTGTTGGGGGCTATCTTC-3': D_6-esRAGE, forward 5'-ctcgagCCAGGACCCTGGAAGGAAGCAGGA-3' and reverse 5'-tctagattaatcatcgtcgtcatcgtcggcctctgcttcaccggtCATGTGTTGGGGGCTATCTTC-3': D_{10}-esRAGE, forward 5'-ctcgagCCAGGACCCTGGAAGGAAGCAGGA-3' and reverse 5'-tctagattagtcgtcgtcgtcatcatcgtcgtcatcgtcggcctctgcttcaccggtCATGTGTTGGGGGCTATCTTC-3': D_{14}-esRAGE, forward 5'-ctcgagCCAGGACCCTGGAAGGAAGCAGGA-3' and reverse 5'-tctagattaatcatcatcatcgtcgtcgtcgtcatcatcgtcgtcatcgtcggcctctgcttcaccggtCATGTGTTGGGGGCTATCTTC-3'. The nucleotide sequences compatible with 6, 10 or 14 L-Asp were added to the reverse primers used here. The amplified cDNAs were cloned and sequenced. The cDNAs were then transferred into *Xho*I–*Xba*I cloning sites of mammalian expression vector pcDNA3.1 (+).

The esRAGE, D_6-esRAGE, D_{10}-esRAGE and D_{14}-esRAGE cDNAs subcloned in pcDNA3.1 (+) were then transfected into Chinese hamster ovary (CHO-K1) cells with Lipofectamine 2000 according to the manufacturer's instruction. Selection of colonies was carried out in growth medium with DMEM supplemented with 10% heat-inactivated fetal bovine serum (FBS), plus 400 µg/mL G418 for 10–12 d. Individual clones were picked, grown to confluency and analyzed for protein expression by Western blot analysis in the medium as described below. The highest-producing clone was grown in collection medium with EX-CELL® 325 PF CHO Serum-Free Medium for CHO Cells (protein free) and 10% heat-inactivated FBS. When the cells reached confluency, the cells were rinsed with PBS and fed with collection medium without FBS to collect protein for further experiments.
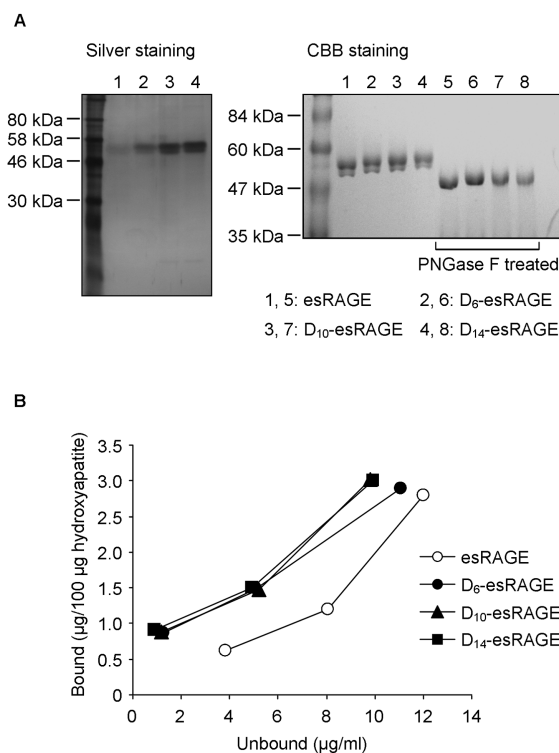

Figure 1. (A) The purified proteins (1 or 2 µg) were subjected to SDS-PAGE under reducing condition and stained with silver or CBB, respectively. Two bands appeared in all the proteins (lanes 1–4). Molecular masses of the untagged esRAGE (lane 1) were approximately 49 and 52 kDa, while those of D_6-esRAGE, D_{10}-esRAGE and D_{14}-esRAGE were larger (lanes 2–4). For digestion of N-linked oligosaccharides, 2 µg each of the untagged and tagged proteins was denatured in denaturing buffer (0.5% SDS and 40 mmol/L dithiothreitol) at 100°C for 3 min, and the denatured proteins were then treated with 500 units of PNGase F in reaction buffer (50 mmol/L sodium phosphate (pH 7.5) and 1% NP-40) at 37°C for 1 h. The PNGase F–treated proteins were analyzed by SDS-PAGE after CBB staining. The PNGase F–treated protein showed a single band and smaller molecular mass than the untreated protein (lanes 5–8). (B) The purified proteins were mixed with HA suspension at a final concentration of 10, 20 and 40 µg/mL. The unbound protein was separated from the bound protein by centrifugation, and the concentration of unbound protein in the supernatant was measured by Western blot analysis. The amount of bound protein was calculated by subtracting the unbound from the total. The longer acidic oligopeptide tagging showed the higher binding affinity of esRAGE to HA.

Purification of Recombinant Proteins

The esRAGE, D_6-esRAGE, D_{10}-esRAGE and D_{14}-esRAGE proteins were purified by a three-step column procedure. To determine the desired protein-containing fractions in each step, the eluted fractions were analyzed by using sodium dodecyl sulfate–polyacrylamide gel electrophoresis (SDS-PAGE), followed by coomassie brilliant blue (CBB) staining. Unless stated otherwise, all steps were performed at 4°C.

Step 1. The medium containing each of the untagged and acidic oligopeptide–tagged esRAGE protein was filtered through a 0.2-µm filter and then dialyzed against 25 mmol/L Tris buffer (pH 7.5) by using a Vivacell 70 centrifugal filter device.

Step 2. The dialyzed medium was applied to a column of DEAE–Sepharose equilibrated with 25 mmol/L Tris buffer (pH7.5). The column was first washed with 25 mmol/L Tris buffer (pH 7.5),

and then the protein was eluted with 0–0.8 mol/L NaCl in a linear gradient.

Step 3. The eluted fractions containing the desired protein were pooled and dialyzed against 25 mmol/L Tris buffer (pH 7.5) by using a Vivaspin 15 centrifugal filter device.

Step 4. The dialyzed fractions were applied to a column of Heparin Sepharose equilibrated with 25 mmol/L Tris buffer (pH 7.5). The column was washed with 25 mmol/L Tris buffer (pH 7.5), and then the protein was eluted with 0–1.0 mol/L NaCl in a linear gradient.

Step 5. The eluted fractions containing the desired protein were pooled and dialyzed against phosphate-buffered saline (PBS) (pH 7.4) by using a Vivaspin 15 centrifugal filter device. The dialyzed fractions were then concentrated for step 6.

Step 6. The concentrated fractions were applied to a column of Sephacryl S-300-HR equilibrated with PBS. The protein was eluted with PBS.

Step 7. The eluted fractions containing the desired protein were pooled and concentrated after removal of endotoxin by using Detoxi-gel endotoxin removal gel. The concentrated fractions were stored at –80°C until use.

Western Blot Analysis

An analyte was subjected to SDS-PAGE and transferred to a polyvinylidene difluoride membrane. The membrane was probed with primary anti-RAGE antibody, followed by incubation with horseradish peroxidase–conjugated anti-rabbit IgG as a secondary antibody. Blots were developed with an ECL Plus kit and scanned using Typhoon 9410 (GE Healthcare).

Hydroxyapatite-Binding Assay

HA beads were suspended in 50 mmol/L Tris-buffered saline, pH 7.4, at a concentration of 100 µg/100 µL. The purified esRAGE, D_6-esRAGE, D_{10}-esRAGE and D_{14}-esRAGE were mixed with the HA suspension at final concentrations of 10, 20 and 40 µg/mL. The mixtures were agitated at 37°C for 1 h, followed by centrifugation at 12,000g for 5 min to cap-

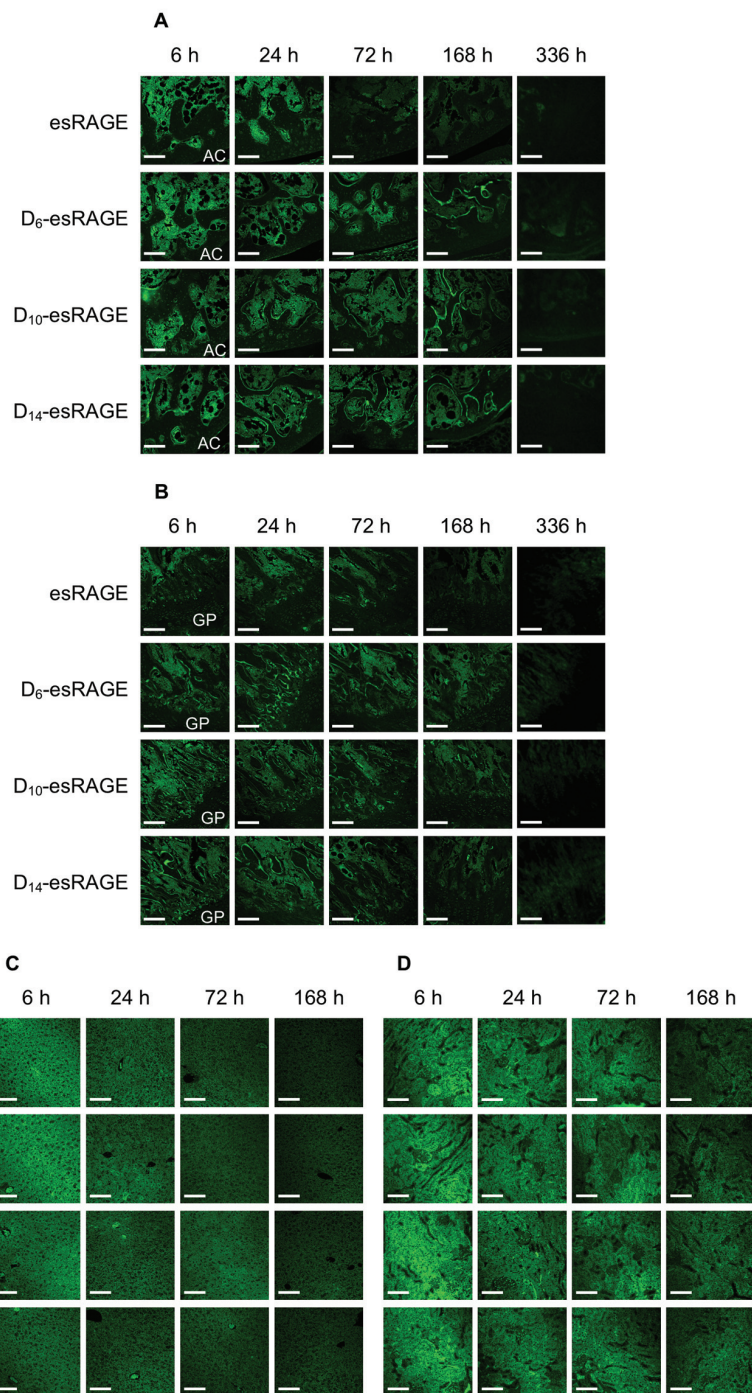**Figure 2.** Biodistribution of fluorescence-labeled esRAGE, D_6-esRAGE, D_{10}-esRAGE and D_{14}-esRAGE to bone. The fluorescence-labeled proteins were injected into mice via the tail vein at a dose of 1 mg/kg body weight. At the indicated time points, the legs, liver and kidney were dissected and sectioned. The sections were observed under a confocal laser scanning microscope to evaluate the distribution of each esRAGE at the femoral epiphysis (A), metaphysis (B), liver (C) and kidney (D). Untagged and tagged esRAGEs were distributed in bone marrow but not in articular cartilage or in growth plate. Only the tagged esRAGEs were additionally distributed and retained in the mineralized region. AC, articular cartilage; GP, growth plate; scale bar = 100 µm.

ture the esRAGE-bound HA beads. The supernatants were analyzed by Western blot analysis to determine the amount of unbound esRAGE. The intensity of immunoreactive blots was quantified by using ImageQuant TL software (GE Healthcare). The concentration of untagged or acidic oligopeptide–tagged esRAGE in the supernatant was estimated from the separately established calibration curve containing the corresponding untagged and tagged esRAGEs in the range from 1.25 to 10 µg/mL. The amount of esRAGE bound to the HA beads was calculated by subtracting the amount of unbound protein from the total amount of esRAGE added to each tube. The dissociation constant (K_d) was determined from double-reciprocal plots.

Tissue Distribution of Untagged and Acidic Oligopeptide–Tagged esRAGE

A total of 1 mg/mL esRAGE, D_6-esRAGE, D_{10}-esRAGE and D_{14}-esRAGE were respectively labeled with Alexa Fluor 488 Protein Labeling Kit following the manufacturer's instructions. The Alexa-labeled esRAGE was injected into DBA/1J mice via the tail vein at a dose of 1 mg/kg body weight. Mice were killed at 6, 24, 72, 168 and 336 h after a single infusion, and legs, liver and kidney were dissected. The tissues were immersion-fixed in 10% neutral buffered formalin, embedded in paraffin and sectioned. Fluorescence images were taken with a confocal laser scanning microscope (LSM 510; Carl Zeiss, Jena, Germany).

Assay for HMGB1 Binding to esRAGE and D_6-esRAGE

According to the results of tissue distribution study, significant difference among acidic oligopeptide–tagged esRAGEs was not observed. Therefore, HMGB1 binding assay was performed for esRAGE and D_6-esRAGE. Nickel affinity gel was suspended in PBS containing 4 mmol/L imidazole at a final concentration of 10 v/v%. A total of 5 µg His-tagged HMGB1 was added into the
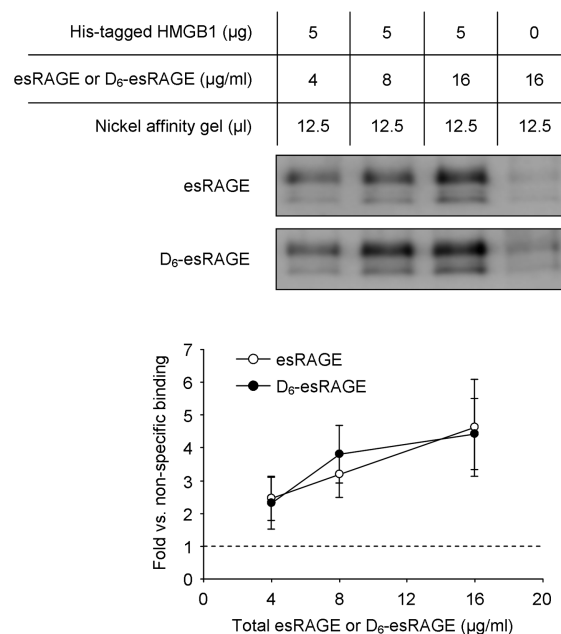

His-tagged HMGB1 (µg)	5	5	5	0
esRAGE or D_6-esRAGE (µg/ml)	4	8	16	16
Nickel affinity gel (µl)	12.5	12.5	12.5	12.5
esRAGE				
D_6-esRAGE				

Figure 3. Concentration-dependent binding curves of esRAGE and D_6-esRAGE to HMGB1. His-tagged HMGB1 was incubated and immobilized to Nickel affinity gel suspension in PBS containing 4 mmol/L imidazole, and esRAGE or D_6-esRAGE was then added to the suspension at a final concentration of 4, 8 and 16 µg/mL. The mixture was agitated at 37°C for 30 min to allow the binding of esRAGE and D_6-esRAGE to HMGB1 immobilized in Nickel affinity gel. After washing the Nickel affinity gel with PBS containing 4 mmol/L imidazole, the bound esRAGE and D_6-esRAGE was eluted from the gel complex by incubating in PBS containing 250 mmol/L imidazole. The eluted esRAGE and D_6-esRAGE was determined by Western blot analysis and the relative intensities of immunoreactive blots were calculated. The concentration-dependent binding curves were comparable between esRAGE and D_6-esRAGE. Each point with a bar represents the mean ± standard deviation (SD) of three experiments.

nickel affinity gel suspension. The purified esRAGE and D_6-esRAGE were respectively mixed with the suspension and agitated at 37°C for 30 min, in which gel complexes composed of nickel affinity gel, His-tagged HMGB1 and esRAGE or D_6-esRAGE were allowed to form. The mixtures were centrifuged at 6,000*g* for 1 min to capture the gel complexes, and the gel complexes were washed three times with PBS containing 4 mmol/L imidazole. The gel complexes were agitated in PBS containing 250 mmol/L imidazole for 5 min to elute the esRAGE and D_6-esRAGE from the gel complexes. After centrifugation at 6,000*g* for 1 min, the supernatants were analyzed by Western blot analysis to determine esRAGE and D_6-esRAGE bound to His-tagged HMGB1.

Mouse Monocyte/Macrophage Cell Culture

According to the results of the tissue distribution study, a significant difference between acidic oligopeptide–tagged esRAGEs was not observed. Therefore, esRAGE and D_6-esRAGE were used to test the effect on TNF-α production into cell culture medium. RAW264.7 cells were suspended in DMEM supplemented with 10% heat-inactivated FBS and seeded at 2×10^4 cells/well in a 96-well plate. At 24 h after the seeding, the cells were treated with the indicated concentration of HMGB1 in the presence or absence of esRAGE and D_6-esRAGE. The cell culture medium was collected with the indicated time intervals after the HMGB1 treatment, and level of TNF-α in the medium was determined by using the ELISA kit.

Murine Model of Bovine Collagen Type II–Induced Arthritis

Six-week-old DBA/1J mice were housed in a room maintained at 24.5 ± 0.5°C on a 12:12-h light–dark cycle. They were allowed to acclimate for 1 wk before the start of experiments and free access to food and water. On d 0, the mice weighing 20–30 g were treated at the base of the tail intradermally with 150 μg bovine collagen type II dissolved in 0.1 mol/L acetic acid and emulsified in CFA. On d 21, the mice were challenged by subcutaneous injection of 150 μg bovine collagen type II in IFA (32,33). At 14 d after primary immunization, the mice were treated with esRAGE (1.0 mg/kg per week) or D_6-esRAGE (1.0 mg/kg per week) intraperitoneally. Vehicle treatment (control) consisted of 100 μL PBS. Treatment was continued weekly in a total of three weekly injections, and mice were killed on d 34 after primary immunization. Arthritis was evaluated semiquantitatively by clinical and histopathological scoring in a blinded manner.

Clinical severity of arthritis was characterized by palpation and observations of joint properties and inflammation of surrounding tissues in each limb. The arthritis was graded on a scale of 0–3, using the previously published scoring system (34): 0 = normal, 1 = slight swelling and/or erythema of the fingers, 2 = pronounced edematous swelling and 3 = joint rigidity with edematous swelling or joint ankylosis. Scores of 1 and 2 mainly reflect reversible edematous inflammation, but a score of 3 reflects irreversible components such as established joint ankylosis. All four limbs were investigated, providing a maximum score of 12 per mouse as a cumulative grade.

Histopathological severity of arthritis was characterized by synovial lesion, cartilage destruction and bone destruction on hematoxylin and eosin (H&E)-stained sections and Safranin O–stained sections of knee joints. Severity of arthritis was assessed in a blinded manner by two independent investigators

Figure 4. HMGB1-induced TNF-α secretion in RAW264.7 cells and blockade of TNF-α secretion by esRAGE and D_6-esRAGE. (A) RAW264.7 cells were stimulated with the indicated concentration of HMGB1, and ELISA was used to measure the level of TNF-α secreted into the conditioned medium. TNF-α was secreted in a concentration-dependent manner for 24 h after stimulation with HMGB1, and TNF-α level peaked at 6 h and then tended to decrease. Each point with a bar represents the mean ± SD of three experiments. (B) RAW264.7 cells were treated with the indicated concentration of esRAGE or D_6-esRAGE for 1 h, and the cells were then treated with 3 μg/mL HMGB1 for 6 h, followed by measurement of TNF-α level in the conditioned medium. Secretion of TNF-α was significantly inhibited by esRAGE or D_6-esRAGE at a concentration of 3 μg/mL. Each column with a bar represents the mean ± SD of three experiments. **Significantly different from HMGB1-untreated control at $P < 0.01$. #Significantly different from HMGB1-treated control at $P < 0.05$.

on a scale of 0–3, by using the following scoring system (35): synovial lesions: 0 = no lesions, 1 = mild effect, 2 = moderate effect/proliferation, and 3 = severe lesions with destruction; cartilage destruction: 0 = none, 1 = mild destruction of superficial cartilage, 2 = moderate destruction, and 3 = severe destruction with loss or complete fragmentation of cartilage; bone destruction: 0 = none, 1 = mild destruction of subchondral bone, 2 = moderate destruction, and 3 = severe destruction with loss of large areas of bone.
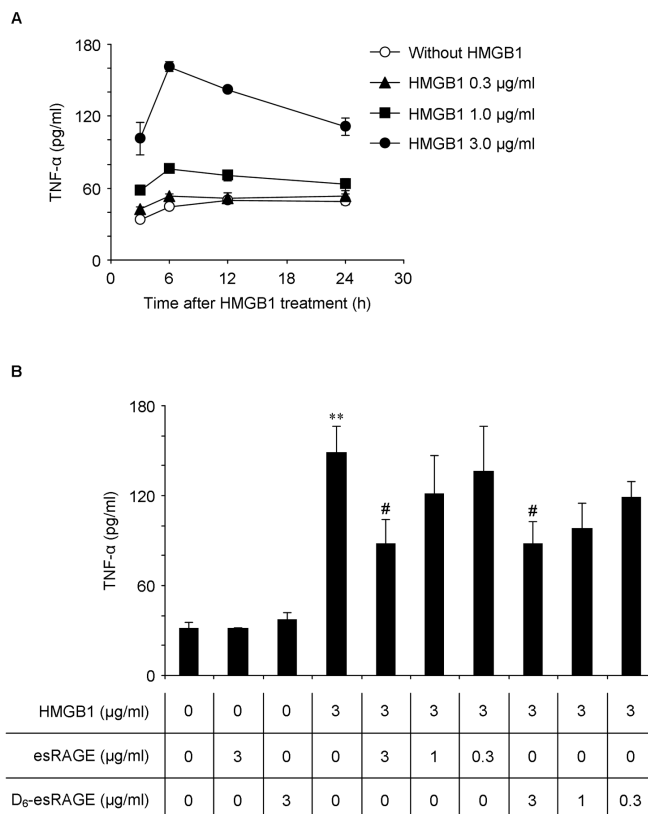
Statistical Analysis

Statistical analysis was performed using one-way analysis of variance followed by the Tukey-Kramer *post hoc* test. Differences were considered to be significant at $P < 0.05$.

RESULTS

Characterization of Untagged and Acidic Oligopeptide–Tagged esRAGEs

Untagged esRAGE was endogenously truncated at the C-terminus, which is involved in membrane penetration, and

was accordingly secreted into the culture medium when stably expressed in CHO-K1 cells. The acidic oligopeptide–tagged esRAGEs (D_6-esRAGE, D_{10}-esRAGE and D_{14}-esRAGE), in which a stretch of acidic oligopeptide was introduced at C-terminus of esRAGE, were secreted into the culture medium as well. The secreted amounts of esRAGE, D_6-esRAGE, D_{10}-esRAGE and D_{14}-esRAGE into the culture medium were 4.26, 5.93, 2.93 and 2.97 mg, respectively, per liter of the medium in 24 h. Their purification yields were 19.2, 32.6, 33.4 and 30.1%, respectively. Since the ligand-binding site of esRAGE locates on V-region close to N-terminus, the acidic oligopeptide stretch was tagged into C-terminus to avoid influence for ligand binding. When the purified esRAGE was subjected to SDS-PAGE under reducing conditions followed by silver staining and CBB staining, two protein bands with molecular mass of approximately 49 and 52 kDa were detected (Figure 1A). Silver staining was less sensitive than CBB staining for the detection of esRAGE. The purified esRAGE was also analyzed by Western blot by using polyclonal antibody against RAGE. The resultant immunoreactive two protein bands showed the same molecular mass as those of CBB staining (data not shown). The deduced increase in molecular mass associated with the stretch of acidic oligopeptide and TGEAEA spacer, for which the nucleotide sequence (5'-accggtgaagcagaggcc-3') was introduced to create an *Age*I cleavage site for cloning purpose, was observed with D_6-esRAGE, D_{10}-esRAGE and D_{14}-esRAGE (Figure 1A).

esRAGE has two potential N-glycosylation sites (20). We examined whether the two protein bands have this type of modification and are derived from variants of N-linked oligosaccharides by using PNGase F, which specifically cleaves off oligosaccharides attached to asparagine residues. When the purified untagged esRAGE was treated with PNGase F, two protein bands with molecular masses of approximately 49 and 52 kDa disappeared, and one new band appeared at approximately 46 kDa, indicating that the
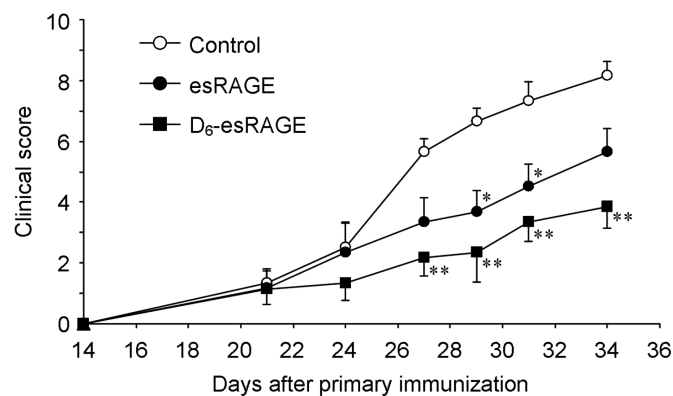
untagged esRAGE was modified with two major variants of N-linked oligosaccharides (Figure 1A). The tagged esRAGE showed the same trend as the untagged esRAGE.

Because the action of acidic oligopeptide as a bone-targeting carrier attributes to binding affinity to HA, we examined the binding affinity of the untagged and tagged esRAGEs to HA *in vitro*. The binding parameter, K_d, of tagged esRAGEs was approximately 20-fold lower than that of untagged RAGE (esRAGE, 47.8 µg/mL; D_6-esRAGE, 2.6 µg/mL; D_{10}-esRAGE, 3.0 µg/mL; D_{14}-esRAGE, 1.6 µg/mL), meaning the affinity of tagged esRAGEs to HA was greater than that of untagged esRAGE. However, no significant difference was observed between the tagged esRAGEs forms (Figure 1B).

Biodistribution of Untagged and Acidic Oligopeptide–Tagged esRAGE

The biodistribution of the untagged and tagged esRAGEs was evaluated after a single injection of fluorescence-labeled esRAGE, D_6-esRAGE, D_{10}-esRAGE and

D_{14}-esRAGE at a dose of 1 mg/kg. Figure 2 shows the histological pictures of biodistribution of these esRAGEs at femoral epiphysis and metaphysis at 6, 24, 72, 168 and 336 h after a single intravenous injection. At 6 h, the untagged and tagged esRAGEs were equally distributed in bone marrow but were detected neither in articular cartilage nor in growth plate. However, the tagged esRAGEs were distributed to the mineralized region. At 72 h, the untagged esRAGE almost disappeared from the bone marrow, while the tagged esRAGEs were retained in the bone marrow and mineralized region. Moreover, the tagged esRAGEs were detectable until 168 h, especially at the mineralized region, and almost disappeared from the mineralized region at 336 h. The difference between the tagged esRAGEs forms was observed only at 168 h; D_{10}-esRAGE and D_{14}-esRAGE showed a slightly higher retention than D_6-esRAGE at the mineralized region of the epiphysis. The distribution of untagged and tagged esRAGEs in liver and kidney was also evaluated. In liver, the distribution was widespread

Figure 5. Suppressive effects of esRAGE and D_6-esRAGE on inflammation in DBA/1J mice immunized with bovine collagen type II. At the indicated time points after primary immunization with bovine collagen type II, clinical scoring was performed by blinded observers. Administration of esRAGE and D_6-esRAGE started on d 14 after the immunization when mice initially developed the sign of arthritis such as paw swelling. Each esRAGE and D_6-esRAGE was intraperitoneally administered at a dose of 1 mg/kg per week. esRAGE ameliorated the increase in clinical score, while D_6-esRAGE showed more significant reduction in clinical score than esRAGE from d 27 after primary immunization onward. Each point with a bar represents the mean ± standard error of the mean (SEM) of six mice. *Significantly different from vehicle-treated immunized mice (control) at $P < 0.05$. **Significantly different from vehicle-treated immunized mice (control) at $P < 0.01$.

throughout the liver, including hepatocytes and sinus-lining cells. The distribution patterns in the liver were comparable between the untagged and tagged esRAGEs (Figure 2C). In kidney, no significant differences were also observed between the untagged and tagged esRAGEs (Figure 2D). At 336 h, the untagged and tagged esRAGEs were undetectable in liver and kidney (data not shown). A significant difference between acidic oligopeptide–tagged esRAGEs was not observed in the biodistribution. In addition, it is likely that a longer stretch of acidic oligopeptide affects physiological properties, except for biodistribution of esRAGE, because Nishioka *et al.* (27) demonstrated that the longer stretch of acidic oligopeptide more largely changed the N-linked oligosaccharides structure of glycoprotein. The ligand-binding V-domain of RAGE contains two potential N-glycosylation sites, and the N-linked oligosaccharides on RAGE are suggested to mediate the interaction with its ligands (20,21). It was predicted that the longer stretches, D_{10} and D_{14}, tagged into esRAGE may affect the binding affinity to its ligands. Taken together, we decided to use D_6-esRAGE for further experiments.

HMGB1-Binding Affinity of esRAGE and D_6-esRAGE

We examined the binding affinity of esRAGE and D_6-esRAGE to HMGB1, which is one of the endogenous ligands for RAGE. Each purified esRAGE and D_6-esRAGE was incubated with the His-tagged HMGB1 immobilized to nickel-affinity gel. Figure 3 shows that esRAGE bound to HMGB1 in a concentration-dependent manner consistent with the previous study (36). D_6-esRAGE showed the same trend in binding affinity to HMGB1 as that of esRAGE. It is reasonable that the ability of D_6-esRAGE to bind to HMGB1 ligand was comparable to that of esRAGE, since the site to engage HMGB1 ligand resides in the N-terminal V domain, which both esRAGE and D_6-esRAGE possess.
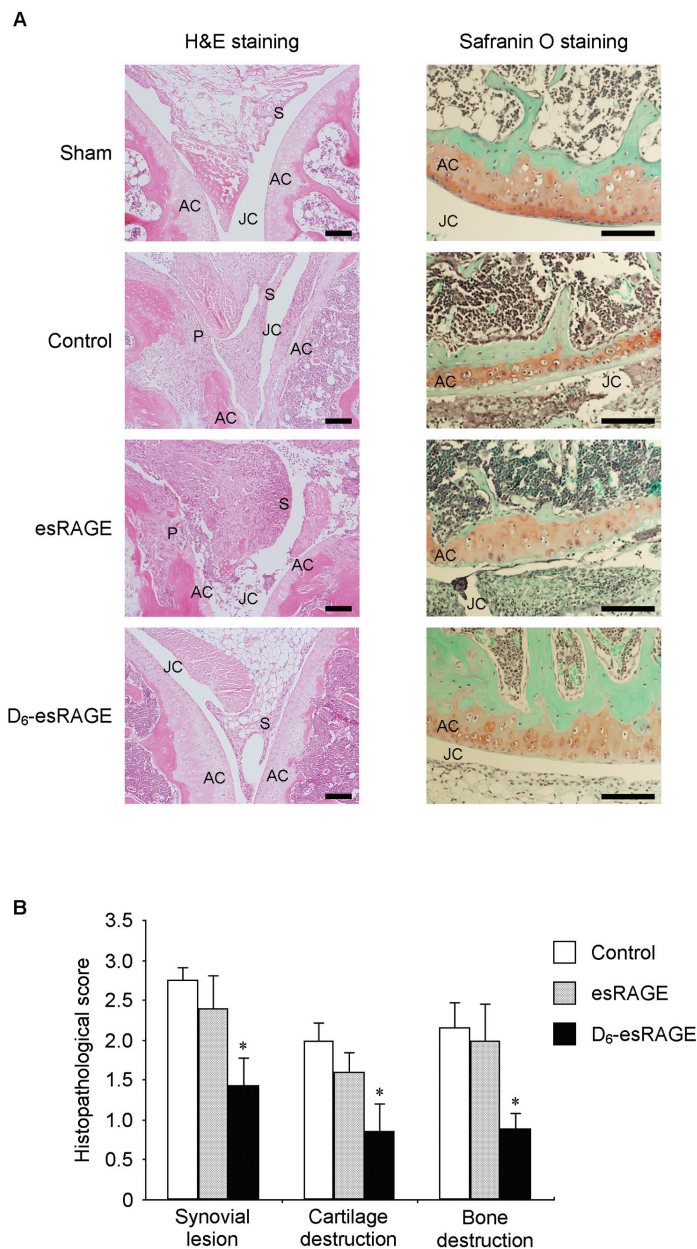

Figure 6. Suppressive effects of D_6-esRAGE, but not esRAGE, on histopathological abnormalities in knee joints of mice immunized with bovine collagen type II. Treatment of each esRAGE and D_6-esRAGE started to be administered intraperitoneally at a dose of 1 mg/kg per week on d 14 after primary immunization. (A) On d 34, the legs of immunized mice were dissected and sectioned, followed by H&E staining and Safranin O staining. (B) To assess the histopathological severity of arthritis focusing on synovial hyperplasia, cartilage destruction and bone destruction, histopathological scoring was performed in a blinded manner. D_6-esRAGE provided an impact to reduce the histopathological scores on synovial lesion (disappearance of hyperplasia), cartilage destruction (smooth surface of organized articular cartilage) and bone destruction, whereas esRAGE did not show any significant preventive effect on histopathological abnormalities. Each column with a bar represents the mean ± SEM of six mice. *Significantly different from vehicle-treated immunized mice (control) at $P < 0.05$. AC, articular cartilage; JC, joint cavity; P, pannus; S, synovium; scale bar = 100 μm.

Blockade of HMGB1-Induced TNF-α Secretion by esRAGE and D_6-esRAGE

The previous study demonstrated that HMGB1 interacts with cell surface TLR-2 and TLR-4 on RAW264.7 cells and activates downstream signals (37). To clarify the potential ability of esRAGE and D_6-esRAGE to function as a decoy receptor, we investigated whether esRAGE and D_6-esRAGE could inhibit the HMGB1-induced TNF-α secretion by RAW264.7 cells. RAW264.7 cells were stimulated with HMGB1, and the level of TNF-α secreted into conditioned medium was measured by ELISA. The peak TNF-α level after stimulation with HMGB1 occurred at 6 h and tended to decrease after 24 h. TNF-α was secreted in a concentration-dependent manner at each time point after stimulation with HMGB1 (Figure 4A). In the presence of esRAGE or D_6-esRAGE, TNF-α secretion induced by 3 μg/mL HMGB1 was down-regulated in a concentration-dependent manner and significantly inhibited at a concentration of 3 μg/mL esRAGE or D_6-esRAGE (Figure 4B).

Therapeutic Effects on Murine Collagen-Induced Arthritis by esRAGE and D_6-esRAGE

DBA/1J mice were immunized with bovine type II collagen in CFA and then boosted with bovine type II collagen in IFA on d 21 after primary immunization. Vehicle (PBS), esRAGE (1.0 mg/kg) or D_6-esRAGE (1.0 mg/kg) was administered to the immunized mice intraperitoneally once a week from d 14 after primary immunization, when the clinical signs of collagen-induced arthritis (CIA) first appeared. To determine and compare the anti-arthritic effect of esRAGE and D_6-esRAGE, clinical score was assessed three times a week. After 2–3 wks after the first injection of bovine type II collagen, mice developed paw swelling. Vehicle-treated immunized mice (control) displayed significant increase in the clinical arthritis score when compared with nonimmunized mice (sham), but arthritis progression and severity were prevented in the esRAGE- and
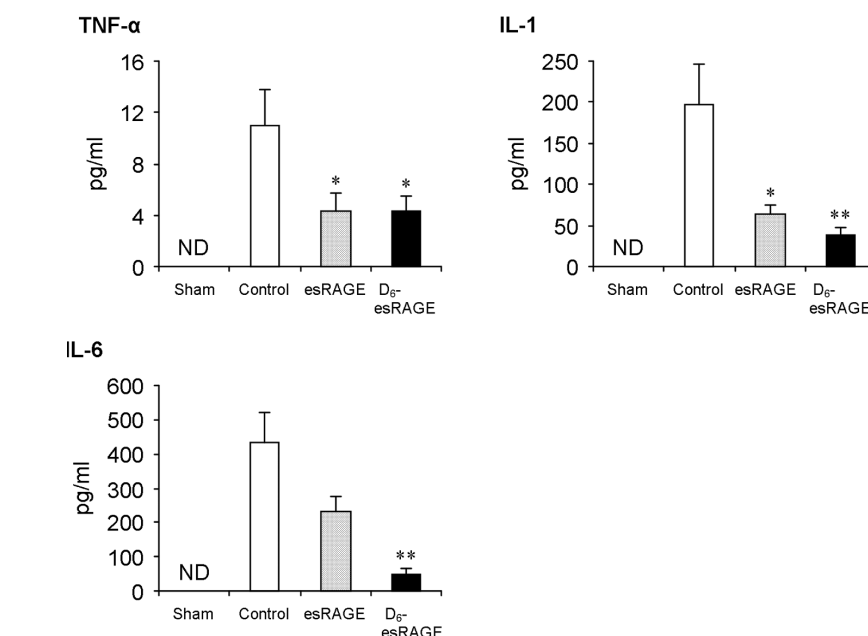

Figure 7. Suppressive effects of esRAGE and D_6-esRAGE on generation of proinflammatory cytokines including TNF-α, IL-1 and IL-6 in plasma of mice immunized with bovine collagen type II. Treatment of each esRAGE and D_6-esRAGE started to be administered intraperitoneally at a dose of 1 mg/kg per week on d 14 after primary immunization. On d 34, plasma of immunized mice was collected before sacrifice and levels of TNF-α, IL-1 and IL-6 in plasma were measured by ELISA. The elevated TNF-α level in immunized mice was suppressed at the same degree in both esRAGE- and D_6-esRAGE–treated groups. The elevated plasma levels of IL-1 and IL-6 were more suppressed by D_6-esRAGE than esRAGE. Each column with a bar represents the mean ± SEM of six mice. *Significantly different from vehicle-treated immunized mice (control) at $P < 0.05$. **Significantly different from vehicle-treated immunized mice (control) at $P < 0.01$. ND, not detected.

D_6-esRAGE–treated immunized mice. The preventive effect was observed even in esRAGE-treated mice, although D_6-esRAGE–treated mice showed further lower clinical scores at all time points, suggesting the more clinical improvement compared with esRAGE-treated mice (Figure 5).

In histopathological evaluation by H&E staining and Safranin O staining, the knee joints of the untreated control mice evidenced notable synovial hyperplasia, depletion of proteoglycan and chondrocytes in articular cartilage, and bone destructions (Figure 6A). Treatment of D_6-esRAGE markedly attenuated these histopathological findings ($P < 0.05$). However, esRAGE-treated mice did not show any significant preventive effect on histopathological abnormalities (synovial lesion, $P = 0.7405$; cartilage destruction,

$P = 0.6100$; bone destruction, $P = 0.9299$) (Figure 6B).

At the end of the experimental period, the levels of TNF-α, IL-1 and IL-6 in plasma were significantly elevated in untreated control CIA mice compared with sham mice ($P < 0.001$) (Figure 7). Treatment with esRAGE suppressed the elevation of levels of TNF-α and IL-1 observed in untreated CIA mice ($P < 0.05$), but reduction of IL-6 level was not significant in esRAGE-treated mice ($P = 0.0959$). Meanwhile, D_6-esRAGE reduced the levels of all these proinflammatory cytokines ($P < 0.05$), including IL-6, and production of IL-1 and IL-6 was more reduced when compared with esRAGE.

DISCUSSION

We have demonstrated here that the current approach using D_6-esRAGE ame-

liorates the characteristic pathological features on murine CIA. In the pathological process of RA, HMGB1 appears to be a key signal transduction ligand of TLR-2, TLR-4 and RAGE and is implicated in amplification of proinflammatory responses. Accumulation of HMGB1 in synovial fluids and serum of subjects with RA has been correlated with disease severity (9). These findings suggested that neutralization of the interactions between HMGB1 and the cell surface receptors via a soluble decoy receptor, sRAGE, is a potential therapeutic agent for RA. Hofmann *et al.* (38) reported that sRAGE administration ameliorates the clinical and histopathological features in murine CIA. However, the dose of administered sRAGE was substantially higher (daily 100 µg/mouse equivalent to weekly 35 mg/kg) compared with other biologics, implying that biological activity of sRAGE is lower and/or that biodistribution of sRAGE is unfavorable for treatment for CIA. Indeed, we observed that a much lower dose of esRAGE (weekly 1 mg/kg) showed little effectiveness on CIA. To resolve this issue and to prove the therapeutic effect of sRAGE, we hypothesized that drug delivery system to bone could be a valuable additive approach. Thus, we attempted to deliver esRAGE to bone by using a bone-targeting system.

It is known that the ligand-binding V-domain of RAGE contains two potential N-glycosylation sites, and PNGase F treatment reduces its molecular mass, indicating that the RAGE is a glycoprotein. In this study, both untagged and acidic oligopeptide–tagged esRAGEs expressed by CHO-K1 cells were highly glycosylated and were modified with two major variants of N-linked oligosaccharides. Both variants of N-linked oligosaccharides on esRAGE and D_6-esRAGE showed a similar binding affinity to HMGB1 ligand. This finding implies that both variants function as a decoy receptor for HMGB1; therefore, we used both variants for further experiments. Recent studies revealed that the S100 protein levels in the serum and synovial fluids correlate with the arthritis severity as
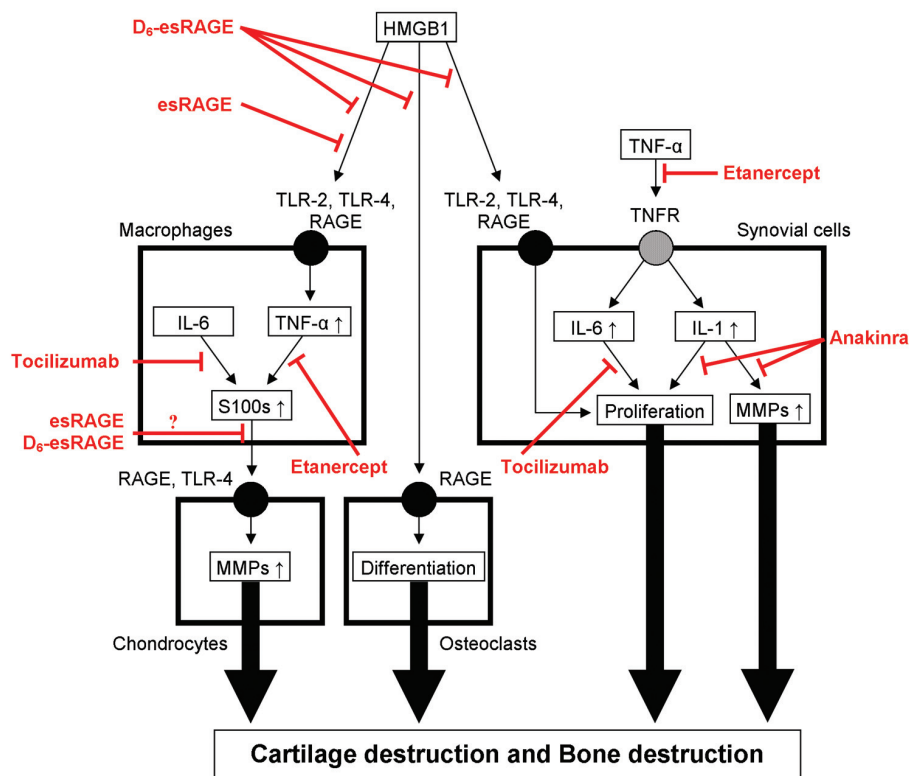

Figure 8. Proposed hypothesis of mechanism of D_6-esRAGE on RA pathogenesis. TNFR, TNF receptor; MMPs, matrix metalloproteinases.

well as HMGB1 (39,40). S100 proteins bind to RAGE and TLR-4 and activate their downstream signals, resulting in increased production of matrix-degrading enzymes, such as matrix metalloproteinases, which are involved in cartilage degradation and progression of RA (41). It is likely that highly glycosylated esRAGE and D_6-esRAGE have binding affinity to S100 proteins, since RAGE enriched for N-linked oligosaccharides shows higher binding affinity to S100 proteins as well as HMGB1 (42,43). Consistently, the binding affinity of diverse ligands such as HMGB1 and S100 proteins to RAGE decreases when RAGE is deglycosylated, indicating that the N-linked oligosaccharides on RAGE mediate the interaction with its ligands (42–44). However, structural influence of N-linked oligosaccharides on RAGE for ligand binding is not completely understood. Further analyses are needed to confirm that esRAGE and D_6-esRAGE bind to ligands other than HMGB1.

A question addressed was whether administered D_6-esRAGE could be delivered to relevant tissues. Pathological lesions in CIA appear not only in bone but also in synovial tissue, which does not contain HA. Consistent with the previous studies (27,28), acidic oligopeptide–tagged esRAGEs, including D_6-esRAGE, were localized to a mineralized region in bone, where they were retained for over 1 week. The principle of bone-targeting by using an acidic oligopeptide is based on the affinity between negatively charged acidic oligopeptide and positively charged calcium in HA. Retention of D_6-esRAGE was not observed in synovial tissue. In addition, D_6-esRAGE was not distributed to avascular regions, such as articular cartilage and growth plate. Despite these facts, why did D_6-esRAGE significantly attenuate the synovial hyperplasia in murine CIA while esRAGE showed little improvement? One can speculate that the prolonged retention of D_6-esRAGE in bone provides a great

chance to infiltrate D_6-esRAGE into synovial tissue or cartilage via synovial fluids. Further pharmacokinetic study in synovial fluids is needed to answer this question.

Cumulative evidence demonstrates that the blockade of TNF-α is effective for patients with RA (5,45,46). Blocking TNF-α has been considered as a therapeutic option for RA treatment. However, in this study, despite substantial reduction of TNF-α level after weekly administration of esRAGE, the esRAGE-treated mice did not show improvement on synovial hyperplasia and bone destruction. This finding indicates that the reduction of TNF-α is insufficient to remit the pathological lesions on murine CIA. Several reports support our finding by proving that severe arthritis appeared in a TNF knockout murine model of CIA (47) and that HMGB1-triggered joint inflammation was observed in TNF knockout mice (48). Thus, even in the absence of TNF, both the inflammatory and destructive components could be induced, resulting in CIA. On the other hand, knockout mice lacking either IL-1 (49) or IL-6 (50) were protected from CIA. Our findings, therefore, provide the additional insights into implication of HMGB1 on TNF-independent mechanisms for RA pathogenesis.

CONCLUSION

We have proven (a) that the blockade of HMGB1 receptor downstream signals by D_6-esRAGE abates synovial hyperplasia, cartilage destruction and bone destruction in CIA through TNF-independent mechanisms (Figure 8) and (b) that the combination of bone-targeting and esRAGE is a potential option for RA treatment.

DISCLOSURE

The authors declare that they have no competing interests as defined by *Molecular Medicine*, or other interests that might be perceived to influence the results and discussion reported in this paper.

REFERENCES

1. Firestein GS. (2003) Evolving concepts of rheumatoid arthritis. *Nature.* 423:356–61.
2. Choy EH, Panayi GS. (2001) Cytokine pathways and joint inflammation in rheumatoid arthritis. *N. Engl. J. Med.* 344:907–16.
3. Feldmann M. (2002) Development of anti-TNF therapy for rheumatoid arthritis. *Nat. Rev. Immunol.* 2:364–71.
4. Maini RN. (2010) Anti-TNF therapy from the bench to the clinic: a paradigm of translational research. *Clin. Med.* 10:161–2.
5. Moreland LW, *et al.* (1999) Etanercept therapy in rheumatoid arthritis: a randomized, controlled trial. *Ann. Intern. Med.* 130:478–86.
6. Cohen S, *et al.* (2002) Treatment of rheumatoid arthritis with anakinra, a recombinant human interleukin-1 receptor antagonist, in combination with methotrexate: results of a twenty-four-week, multicenter, randomized, double-blind, placebo-controlled trial. *Arthritis Rheum.* 46:614–24.
7. Maini RN, *et al.*; CHARISMA Study Group. (2006) Double-blind randomized controlled clinical trial of the interleukin-6 receptor antagonist, tocilizumab, in European patients with rheumatoid arthritis who had an incomplete response to methotrexate. *Arthritis Rheum.* 54:2817–29.
8. Kokkola R, *et al.* (2002) High mobility group box chromosomal protein 1: a novel proinflammatory mediator in synovitis. *Arthritis Rheum.* 46:2598–603.
9. Taniguchi N, *et al.* (2003) High mobility group box chromosomal protein 1 plays a role in the pathogenesis of rheumatoid arthritis as a novel cytokine. *Arthritis Rheum.* 48:971–81.
10. Huttunen HJ, Fages C, Kuja-Panula J, Ridley AJ, Rauvala H. (2002) Receptor for advanced glycation end products-binding COOH-terminal motif of amphoterin inhibits invasive migration and metastasis. *Cancer Res.* 62:4805–11.
11. van Beijnum JR, Buurman WA, Griffioen AW. (2008) Convergence and amplification of toll-like receptor (TLR) and receptor for advanced glycation end products (RAGE) signaling pathways via high mobility group B1 (HMGB1). *Angiogenesis.* 11:91–9.
12. Huang JS, *et al.* (2001) Role of receptor for advanced glycation end-product (RAGE) and the JAK/STAT-signaling pathway in AGE-induced collagen production in NRK-49F cells. *J. Cell. Biochem.* 81:102–13.
13. Zhou Z, *et al.* (2008) HMGB1 regulates RANKL-induced osteoclastogenesis in a manner dependent on RAGE. *J. Bone Miner. Res.* 23:1084–96.
14. Guo HF, *et al.* (2011) High mobility group box 1 induces synoviocyte proliferation in rheumatoid arthritis by activating the signal transducer and activator transcription signal pathway. *Clin. Exp. Med.* 11:65–74.
15. Neeper M, *et al.* (1992) Cloning and expression of a cell surface receptor for advanced glycosylation end products of proteins. *J. Biol. Chem.* 267:14998–5004.
16. Hofmann MA, *et al.* (1999) RAGE mediates a novel proinflammatory axis: a central cell surface receptor for S100/calgranulin polypeptides. *Cell.* 97:889–901.
17. Huttunen HJ, Fages C, Rauvala H. (1999) Receptor for advanced glycation end products (RAGE)-mediated neurite outgrowth and activation of NF-kappaB require the cytoplasmic domain of the receptor but different downstream signaling pathways. *J. Biol. Chem.* 274:19919–24.
18. Malherbe P, *et al.* (1999) cDNA cloning of a novel secreted isoform of the human receptor for advanced glycation end products and characterization of cells co-expressing cell-surface scavenger receptors and Swedish mutant amyloid precursor protein. *Brain Res. Mol. Brain Res.* 71:159–70.
19. Park IH, *et al.* (2004) Expression of a novel secreted splice variant of the receptor for advanced glycation end products (RAGE) in human brain astrocytes and peripheral blood mononuclear cells. *Mol. Immunol.* 40:1203–11.
20. Yonekura H, *et al.* (2003) Novel splice variants of the receptor for advanced glycation end-products expressed in human vascular endothelial cells and pericytes, and their putative roles in diabetes-induced vascular injury. *Biochem. J.* 370:1097–109.
21. Yonekura H, Yamamoto Y, Sakurai S, Watanabe T, Yamamoto H. (2005) Roles of the receptor for advanced glycation endproducts in diabetes-induced vascular injury. *J. Pharmacol. Sci.* 97:305–11.
22. Kasugai S, Fujisawa R, Waki Y, Miyamoto K, Ohya K. (2000) Selective drug delivery system to bone: small peptide (Asp)6 conjugation. *J. Bone Miner. Res.* 15:936–43.
23. Yokogawa K, *et al.* (2001) Selective delivery of estradiol to bone by aspartic acid oligopeptide and its effects on ovariectomized mice. *Endocrinology.* 142:1228–33.
24. Takahashi T, *et al.* (2008) Bone-targeting of quinolones conjugated with an acidic oligopeptide. *Pharm. Res.* 25:2881–8.
25. Oldberg A, Franzén A, Heinegård D. (1986) Cloning and sequence analysis of rat bone sialoprotein (osteopontin) cDNA reveals an Arg-Gly-Asp cell-binding sequence. *Proc. Natl. Acad. Sci. U. S. A.* 83:8819–23.
26. Butler WT. (1989) The nature and significance of osteopontin. *Connect Tissue Res.* 23:123–36.
27. Nishioka T, *et al.* (2006) Enhancement of drug delivery to bone: characterization of human tissue-nonspecific alkaline phosphatase tagged with an acidic oligopeptide. *Mol. Genet. Metab.* 88:244–55.
28. Millán JL, *et al.* (2008) Enzyme replacement therapy for murine hypophosphatasia. *J. Bone Miner. Res.* 23:777–87.

29. Montaño AM, *et al.* (2008) Acidic amino acid tag enhances response to enzyme replacement in mucopolysaccharidosis type VII mice. *Mol. Genet. Metab.* 94:178–89.

30. Tomatsu S, *et al.* (2010) Enhancement of drug delivery: enzyme-replacement therapy for murine Morquio A syndrome. *Mol. Ther.* 18:1094–102.

31. Whyte MP, *et al.* (2012) Enzyme-replacement therapy in life-threatening hypophosphatasia. *N. Engl. J. Med.* 366:904–13.

32. Trentham DE, Townes AS, Kang AH. (1977) Autoimmunity to type II collagen an experimental model of arthritis. *J. Exp. Med.* 146:857–68.

33. Courtenay JS, Dallman MJ, Dayan AD, Martin A, Mosedale B. (1980) Immunisation against heterologous type II collagen induces arthritis in mice. *Nature.* 283:666–8.

34. Williams RO, Feldmann M, Maini RN. (1992) Anti-tumor necrosis factor ameliorates joint disease in murine collagen-induced arthritis. *Proc. Natl. Acad. Sci. U. S. A.* 89:9784–8.

35. Neurath MF, *et al.* (1999) Methotrexate specifically modulates cytokine production by T cells and macrophages in murine collagen-induced arthritis (CIA): a mechanism for methotrexate-mediated immunosuppression. *Clin. Exp. Immunol.* 115:42–55.

36. Hori O, *et al.* (1995) The receptor for advanced glycation end products (RAGE) is a cellular binding site for amphoterin: mediation of neurite outgrowth and co-expression of rage and amphoterin in the developing nervous system. *J. Biol. Chem.* 270:25752–61.

37. Park JS, *et al.* (2006) High mobility group box 1 protein interacts with multiple Toll-like receptors. *Am. J. Physiol. Cell Physiol.* 290:C917–24.

38. Hofmann MA, *et al.* (2002) RAGE and arthritis: the G82S polymorphism amplifies the inflammatory response. *Genes Immun.* 3:123–35.

39. Foell D, *et al.* (2003) Expression of the pro-inflammatory protein S100A12 (EN-RAGE) in rheumatoid and psoriatic arthritis. *Rheumatology (Oxford).* 42:1383–9.

40. Chen YS, Yan W, Geczy CL, Brown MA, Thomas R. (2009) Serum levels of soluble receptor for advanced glycation end products and of S100 proteins are associated with inflammatory, autoantibody, and classical risk markers of joint and vascular damage in rheumatoid arthritis. *Arthritis Res. Ther.* 11:R39.

41. van Lent PL, *et al.* (2008) Stimulation of chondrocyte-mediated cartilage destruction by S100A8 in experimental murine arthritis. *Arthritis Rheum.* 58:3776–87.

42. Turovskaya O, *et al.* (2008) RAGE, carboxylated glycans and S100A8/A9 play essential roles in colitis-associated carcinogenesis. *Carcinogenesis.* 29:2035–43.

43. Srikrishna G, *et al.* (2010) Carboxylated N-glycans on RAGE promote S100A12 binding and signaling. *J. Cell. Biochem.* 110:645–59.

44. Srikrishna G, *et al.* (2002) N-Glycans on the receptor for advanced glycation end products influ-ence amphoterin binding and neurite outgrowth. *J. Neurochem.* 80:998–1008.

45. Lipsky PE, *et al.* (2000) Infliximab and methotrexate in the treatment of rheumatoid arthritis: Anti-Tumor Necrosis Factor Trial in Rheumatoid Arthritis with Concomitant Therapy Study Group. *N. Engl. J. Med.* 343:1594–602.

46. Weinblatt ME, *et al.* (2003) Adalimumab, a fully human anti-tumor necrosis factor alpha monoclonal antibody, for the treatment of rheumatoid arthritis in patients taking concomitant methotrexate: the ARMADA trial. *Arthritis Rheum.* 48:35–45.

47. Campbell IK, O'Donnell K, Lawlor KE, Wicks IP. (2001) Severe inflammatory arthritis and lymphadenopathy in the absence of TNF. *J. Clin. Invest.* 107:1519–27.

48. Pullerits R, Jonsson IM, Kollias G, Tarkowski A. (2008) Induction of arthritis by high mobility group box chromosomal protein 1 is independent of tumour necrosis factor signalling. *Arthritis Res. Ther.* 10:R72.

49. Saijo S, Asano M, Horai R, Yamamoto H, Iwakura Y. (2002) Suppression of autoimmune arthritis in interleukin-1-deficient mice in which T cell activation is impaired due to low levels of CD40 ligand and OX40 expression on T cells. *Arthritis Rheum.* 46:533–44.

50. Alonzi T, *et al.* (1998) Interleukin 6 is required for the development of collagen-induced arthritis. *J. Exp. Med.* 187:461–8.